



EurJOC

European Journal of Organic Chemistry

 **Chemistry
Europe**
European Chemical
Societies Publishing

Accepted Article

Title: Synthesis, Structure and Properties of Fused π -Extended Acridone Derivatives

Authors: Hongshuai Gao and Gang Zhang

This manuscript has been accepted after peer review and appears as an Accepted Article online prior to editing, proofing, and formal publication of the final Version of Record (VoR). This work is currently citable by using the Digital Object Identifier (DOI) given below. The VoR will be published online in Early View as soon as possible and may be different to this Accepted Article as a result of editing. Readers should obtain the VoR from the journal website shown below when it is published to ensure accuracy of information. The authors are responsible for the content of this Accepted Article.

To be cited as: *Eur. J. Org. Chem.* 10.1002/ejoc.202000871

Link to VoR: <https://doi.org/10.1002/ejoc.202000871>

WILEY-VCH

FULL PAPER

Synthesis, Structure and Properties of Fused π -Extended Acridone Derivatives

Hongshuai Gao,^[a] and Gang Zhang*^[a]

[a] Hongshuai Gao, Prof. Dr. Gang Zhang
Jiangsu Co-Innovation Center for Efficient Processing and Utilization of Forest Products, College of Chemical Engineering
Nanjing Forestry University
Longpan Road 159, Nanjing, 210037, P. R. China
E-mail: gangzhang@njfu.edu.cn

Supporting information for this article is given via a link at the end of the document. ((Please delete this text if not appropriate))

Abstract: Benzene- and naphthalene-fused acridone derivatives with hexyl and phenyl groups at the amino position were synthesized and their properties were investigated experimentally and computationally. All the structures of these fused π -extended acridone derivatives were unambiguously confirmed by single crystal X-ray analysis, which revealed the presence of face-to-face π - π stackings along the acridone moiety and the intermolecular hydrogen bond-directed molecular packings of the phenyl substituted acridone derivatives in the crystals. Moreover, the dimerization of linearly fused acridone derivative was observed after storing the crystals over months. The benzene ring at the turning point of the angularly fused acridone derivatives contained relatively longer and shorter C-C bonds, which affected the molecular conjugation, as confirmed by the results of photophysical characterization and the study of the aromaticity. Mobility calculations based on the molecular packings in the single crystals showed that the linearly fused acridone derivatives bearing better electron and hole mobilities are good candidates of organic functional materials.

Introduction

Organic π -conjugated polycyclic heteroaromatic compounds have attracted remarkable attentions not only for the fundamental studies of molecular properties, but also for their potential applications in various electronic devices.^[1] Among the diverse types of heteroatom-doped polycyclic aromatic hydrocarbons, the rigid and planar acridone has recently been realized as an excellent unit in the construction of organic functional materials. Acridone is an anthracene-like tricyclic aromatic compound containing a central pyridone ring with strong fluorescence emission and good photostability.^[2] The benzene rings, the carbonyl and amino positions of acridone are good reaction sites for further functionalization. For example, carbazole and its dendron have been introduced to the benzene rings of acridone to give compounds with thermally activated delayed fluorescence (TADF) behaviour and potential applications in the organic light-emitting diode (OLED) devices.^[3] Diarylamines can couple with the halogenated acridone to form the donor-acceptor system serving as hole-transporting materials in optoelectronic devices.^[4] The conjugation of acridone can be further extended by the formation of acridone oligomer and polymer.^[5] The amino position of acridone can be functionalized with aryl groups to furnish the host materials for OLEDs.^[6] Connecting the electron-withdrawing

anthraquinone to the amino position of acridone, the resulted donor-acceptor system shows TADF feature.^[7] When the rotatable triphenylamine and tetraphenylethene groups are linked to the amino position of acridone, the obtained molecules demonstrate interesting tunable aggregation induced emissions and photoluminescence properties according to the external stimuli.^[8] Stronger electron-withdrawing malononitrile is attached to the carbonyl position of acridone by the formation of C-C double bond to adjust the energy levels of frontier molecular orbitals.^[4a,9] The condensation of cyanoacetic esters and acridone can form molecular rotors with lower rotational barriers due to the generation of donor-acceptor system.^[10] After linking fluorene to the carbonyl of acridone, the acquired molecules demonstrate different kinds of chromisms with respect to the conformational changes.^[11]

All these aforementioned π -conjugated acridone derivatives are synthesized by coupling the functional groups via simple C-C or C-N bonds. But the reports on the π -extended acridone derivatives in the fusion manner are still quite limited.^[12] The π -extension of acridone itself can generate a three dimensional butterfly-shaped polycyclic arene with decreased fluorescence intensity due to the twisted structure.^[12a] Indole can be fused to the benzene ring of acridone to provide an excited-state intramolecular proton transfer (ESIPT) system with potential applications in organic field-effect transistors.^[12b] Two pieces of quinolone are fused to the same benzene ring of acridone to form intramolecular hydrogen bonds between the amine and the neighbouring oxygen atom of carbonyl.^[12c] This novel ESIPT system shows efficient TADF property and has been applied in the high performance OLED devices. Recently our group reported the fusion of the pending benzene ring at the amino position of acridone to form two adjacent pentagon rings can generate interesting concave and boat-shaped polycyclic aromatic hydrocarbons embedded with one or two nitrogen atoms.^[12d,12e] Although there have been other reports on the aromatic rings-fused acridone derivatives, most of them are concerned on the bioactivities and potential pharmaceutical applications without regarding their structural information and optoelectronic properties.^[13]

The pyridone ring in acridone possesses weak aromaticity and the intramolecular charge transfer from nitrogen atom to the carbonyl group can supply the entire molecule with good conjugation. Thus acridone is a promising unit in optoelectronic materials, once its molecular skeleton is further π -extended to

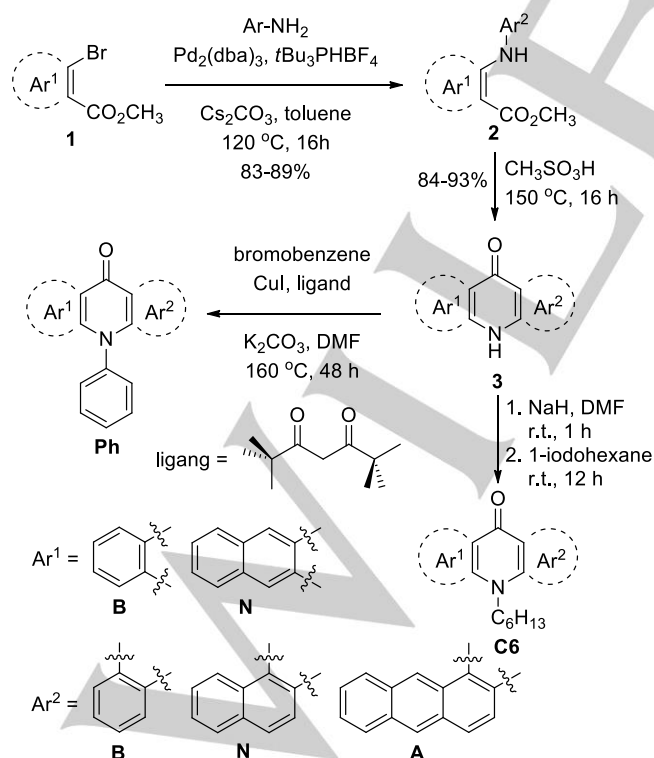
FULL PAPER

narrow the energy gap of the frontier molecular orbitals. We envision that the linear fusion of anthracene-like acridone with benzene and naphthalene may furnish molecules with similar optoelectronic property to that of polycyclic acene.^[14] To explore the property of fused π -extended acridone derivatives and investigate their structure-property relationships, here we report the syntheses and properties of benzene- and naphthalene-fused acridone derivatives with the *N*-substitution by phenyl and hexyl groups.

Results and Discussion

Synthesis

The key step in the synthesis of fused π -extended acridone is the construction of the pyridone ring, which can be achieved by various reported methods.^[15] A convenient way to synthesize acridone is the acid-promoted cyclization of *N*-phenylantranilic acid.^[15a] Based on this consideration, we carried out the synthetic route starting with commercially available methyl 2-bromobenzoate and lab-synthesized methyl 3-bromo-2-naphthoate (Scheme 1). The palladium-catalyzed Buchwald-Hartwig amination of the bromide **1** and the arylamine (aniline, 2-naphthylamine, 2-anthracylamine) with cesium carbonate as the base afforded the intermediates **2** in 83-89% yields. Compound **2** was designed to generate the linear π -extended acridone derivatives after the cyclization of carboxymethyl with the aryl group connecting to the amine to form the pyridone moiety. However, after the cyclization in methanesulfonic acid, the obtained π -extended acridone derivatives **3** were all angular ones with the exception of linear compound **3NB**.



Scheme 1. Synthetic route of the fused π -extended acridone derivatives with phenyl and hexyl at the amine position.

The intramolecular electrophilic cyclization of compounds **2** is regioselective and the reaction always occurs at the 1-position of naphthalene and anthracene. The reason for the formation of angular acridone derivatives rather than the linear ones was studied by density functional theory (DFT) calculations.^[16] Compound **2BN** was taken as an example to explain the reaction pathway (Figure 1). Compared to that of the linear intermediate, the formation of the angular intermediate needs to overcome lower energy barrier and the generated angular intermediate possesses lower potential energy. Thus the intramolecular electrophilic cyclization of compounds **2** prefer to form angular acridone derivatives via the thermodynamically more stable angular intermediate.

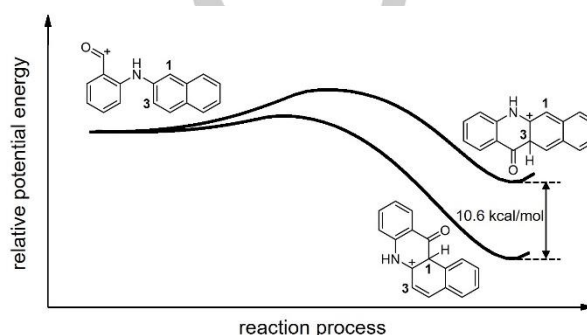
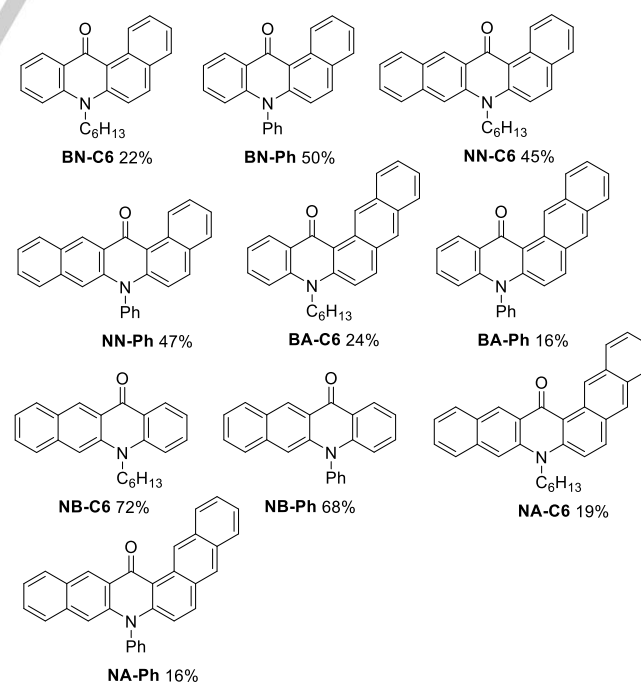


Figure 1. Potential energy diagram for the electrophilic cyclization of **2BN** calculated at the B3LYP/6-311+G (d,p) level of theory.

To improve the solubility of the fused acridone derivatives, compounds **3** were further functionalized at the amino position with either aliphatic hexyl group via nucleophilic substitution, or aromatic phenyl group via copper-catalyzed Ullmann amination to give the final products in low to moderate yields (Scheme 2).



Scheme 2. Structures and yields of the fused π -extended acridone derivatives.

FULL PAPER

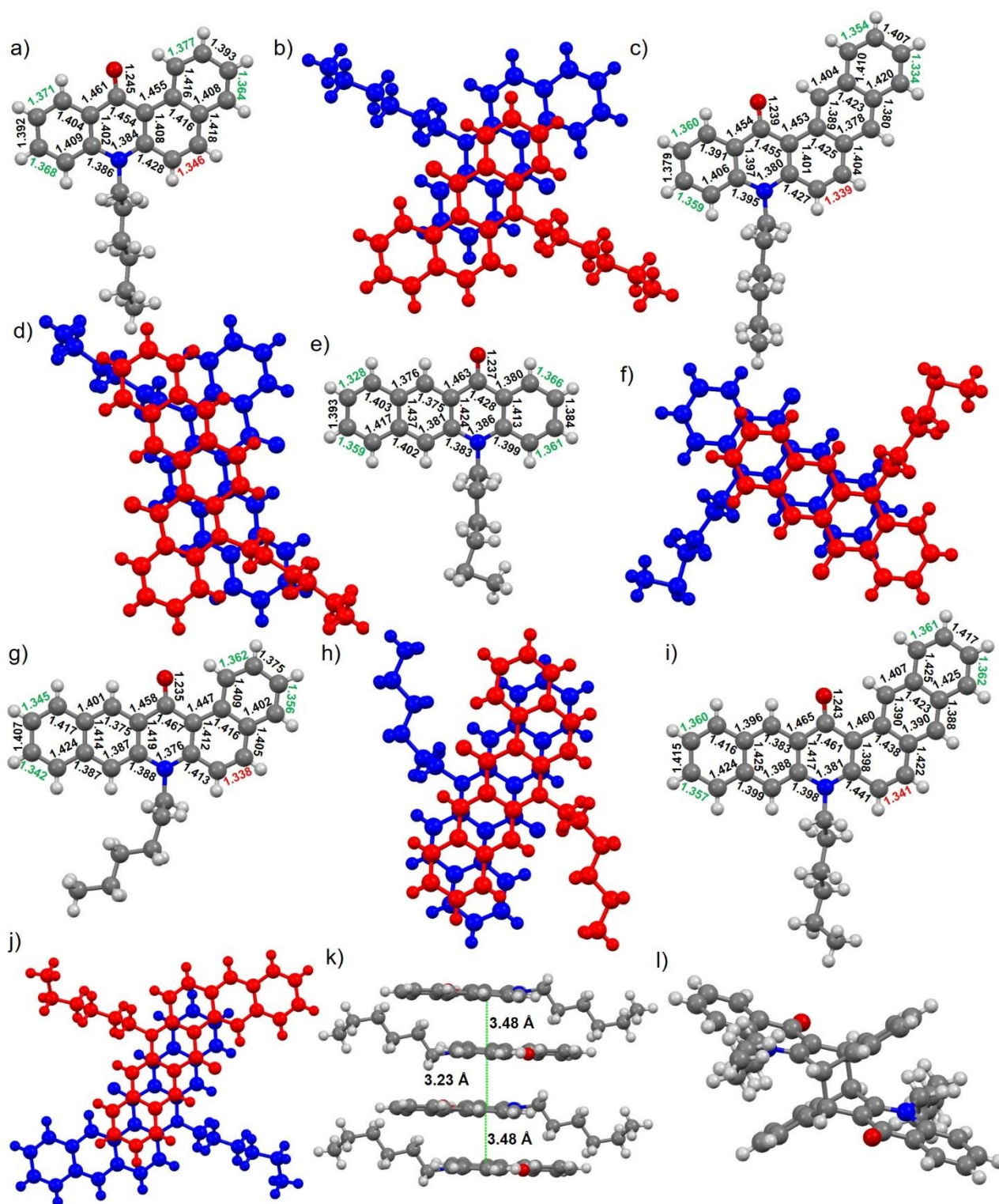


Figure 2. Crystal structures and bond lengths of fused π -extended acridone derivatives with hexyl groups at the amino position: crystal structure and top view of the overlapped molecular π - π stacking in the crystal a, b) **BN-C6**; c, d) **BA-C6**; e, f) **NB-C6**; g, h) **NN-C6**; i, j) **NA-C6**; k) side view of the molecular packing of **NA-C6** formed by π - π interaction with different distances; l) crystal structure of the dimerized **NB-C6**.

Crystal structures and packings

Single crystals that were suitable for X-ray diffraction analysis were obtained for all the target compounds.^[17] The crystals were grown by slow evaporation of the dichloromethane/hexane solutions of **BN-C6**, **BA-C6**, **NB-C6**, **NN-C6**, **BN-Ph**, **NB-Ph**, **NN-**

FULL PAPER

Ph. For **NA-C6**, the crystals were obtained by slow evaporation of its dichloromethane/methanol solution. The vapor diffusion of methanol into the toluene solutions was used to get the crystals of **BA-Ph** and **NA-Ph**. The crystallographic analysis supplied detailed information of the molecular structures and packings in the solid state. For the compounds with hexyl group at the amino position of the π -extended acridone derivatives (Figure 2), the bond lengths of carbonyl in the molecules are in the range of 1.24–1.25 Å, which matches well with that of an acridone dimer with hexyl groups,^[5b] but longer than that of the C–O double bond. The distances of C–C bonds (1.43–1.47 Å) between carbonyl and the adjacent benzene rings and C–N bonds (1.38–1.40 Å) in the molecules are shorter than the lengths of their corresponding single bonds. The alternation of bond lengths in the pyridone moiety clearly demonstrates the delocalization of electron from nitrogen to carbonyl, which can be easily realized when the resonance structures are considered.^[7] The two terminal benzene rings always contain C–C bonds with distances (1.33–1.38 Å) less than that of benzene (1.39 Å), due to the influence of intramolecular charge transfer. Moreover, the outer C–C bond at the turning moiety of the angular acridone derivatives is always short with the lengths in the scale of 1.34–1.35 Å, which are more like the feature of olefin. Whereas the inner one is slightly longer with the distances in the range of 1.44–1.45 Å, close to the length of C–C single bond connecting two sp^2 bonding carbon atoms.^[18] The long and short C–C bond lengths are similar to those of phenanthrene and indicate somewhat different aromaticities in these benzene rings.^[19] The structures of these π -extended acridone derivatives are nearly planar with small dihedral angles of the two terminal benzene rings in the range of 1.7–6.2°.

The rigid aromatic acridone derivatives favor the formation of π - π stacking in the crystals with the distances in the range of 3.35–3.58 Å. The two molecules prefer to be oriented with the hexyl groups directing to the opposite direction in the packing due to the steric hindrance, and overlapped at the linear acridone moiety for compounds **BN-C6**, **NB-C6**, **NN-C6** and **NA-C6**. However, compound **BA-C6** contains three rings at each side and the molecules are packed by overlapping at the central benzene ring with the acridone and anthracene moieties of the two molecules in the *anti* form (Figure 2d). Although π - π stackings between two neighboring molecules are observed, most of them are intermittent and merely involve two molecules due to the interference of flexible hexyl groups. Only compound **NA-C6** demonstrates the consecutive molecular packing via π - π interaction with the layer distances of 3.23 Å and 3.48 Å (Figure 2k).

Intermolecular C–H...O hydrogen bonds of hydrogen atom of the benzene ring at the turning point and oxygen of carbonyl are observed in the crystals of **BN-C6** and **BA-C6** and the dihedral angles of the acridone moieties are 77° and 85°, respectively. The hydrogen atom of the hexyl chain can also form C–H...O intermolecular hydrogen bond with carbonyl in the crystal of **NB-C6**. No hydrogen bonds are formed in the crystal of **NN-C6**. The hydrogen atoms of the methylene linked to the amino position and the terminal benzene ring of anthracene can generate intermolecular C–H...O hydrogen bonds with carbonyl in **NA-C6**.

Multiple C–H... π interactions between the hexyl group and the aromatic rings are observed in all the crystals of the hexyl-substituted acridone derivatives. The flexible hexyl chains partially occupy the acridone surfaces of **BN-C6**, **NB-C6** and **NN-C6**, or lay over the anthracene moiety of **BA-C6**. Such C–H... π interactions keep the adjacent molecules away from forming π - π stackings. For **NA-C6**, C–H... π interactions are also present in the crystal without occupying the aromatic surface, thus leading to a continuous π - π stacking.

It is worthwhile to note that two molecules of linear compound **NB-C6** form uniform π - π stacking with three of the four rings overlapped each other in the crystalline state. In addition to the aforementioned C–H...O and C–H... π interactions among hexyl and acridone moieties, the attractive dispersion interaction between hexyl chains is also involved to keep the π - π stacking from ongoing growth. Furthermore, the X-ray structural analysis of compound **NB-C6** reveals a dimerized structure in the *anti* form after storing the crystals over five months under the ambient laboratory-lighting condition (Figure 2l). The molecules undergo the dimerization process in the crystalline state, which is reasonable considering the well overlapped molecular packing (Figure 2f). To the best of our knowledge, this is the first example of the dimerization of π -extended acridone derivative with the structure confirmed by X-ray diffraction analysis. The dimerization should be caused by the photo-induced cycloaddition, similar to the photodimerization of anthracene and other acenes.^[20] According to the situation of the crystals of non-dimerized **NB-C6**, the dimerization would not happen at least in one week, indicating a very slow decomposition process.

For the phenyl-substituted acridone derivatives, the bond lengths and molecular planarity are close to those of the hexyl-substituted ones. The pending phenyl is nearly vertical to the acridone plane with the dihedral angle in the range of 85–89°. The intermolecular C–H...O hydrogen bond between carbonyl and the hydrogen atoms of the pending benzene ring plays a dominant role in directing the molecular packings, which are also found in the molecular packing of other phenyl-substituted acridone derivatives (Figure 3).^[8c] With the assistance of intermolecular hydrogen bonds, these molecules are well oriented along the acridone moiety. However, the space between atoms of hydrogen and oxygen in such hydrogen bond also makes the acridone planes partially overlapped each other and leads to low degrees of molecular stacking. The formations of intermittent π - π stackings with the distances of 3.51 Å and 3.52 Å are observed in the crystals of **BN-Ph** and **BA-Ph** due to the interference of C–H... π interactions among the neighbouring molecules. Compound **NN-Ph** shows a consecutive overlapped molecular packing with the aid of intermolecular hydrogen bond. Besides the formation of intermolecular C–H...O hydrogen bonds, π - π interactions between molecules are observed in compounds **NB-Ph** and **NA-Ph**, thus leading to the continuous molecular packings along the acridone moiety. The distance between the acridone planes in **NA-Ph** is 3.72 Å, which is slightly longer than the other ones due to the C–H... π interactions between the pending benzene ring and the adjacent anthracene moiety.

FULL PAPER

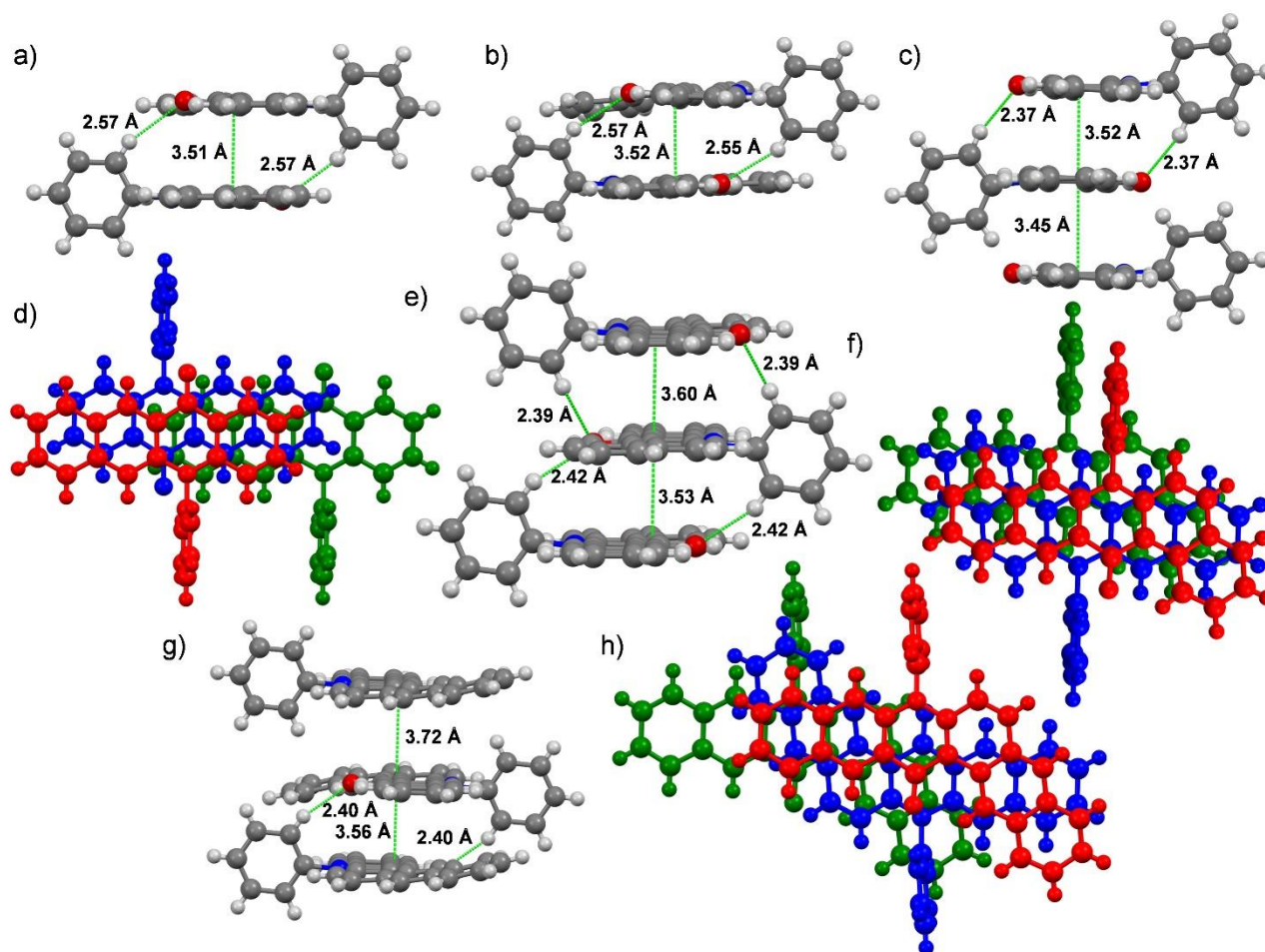


Figure 3. Crystal structures of fused π -extended acridone derivatives with phenyl groups at the amino position: side view of molecular packings via intermolecular hydrogen bond, a) **BN-Ph**; b) **BA-Ph**; side view of the molecular packing and top view of the overlapped molecular structure in the crystal c, d) **NB-Ph**; e, f) **NN-Ph**; g, h) **NA-Ph**.

Optical and electrochemical properties

The optical properties of the fused π -extended acridone derivatives were characterized by UV/vis absorption and fluorescence emission in dichloromethane. For the hexyl-substituted acridone derivatives, the absorption maximum at the longest wavelength is gradually red-shifted from 401 nm for parent *N*-hexylacridone to 484 nm for **NA-C6** due to the extended conjugation (Figure 4, Table 1).^[5b] Compared to that of the angular acridone derivative **BN-C6**, the absorption maximum of the linear isomer **NB-C6** is red-shifted to 467 nm, attributable to the enhanced degree of conjugation. However, even with elongated conjugation, the absorption maximum at the longest wavelength of the angularly fused acridone derivative **NN-C6** is blue-shifted to 461 nm in comparison to that of **NB-C6**. This is possibly due to the steric hindrance caused non-planarity resulting in a reduced conjugation in **NN-C6**. Moreover, the reduced conjugation caused by the longer inner C-C bond at the turning point is also responsible for the blue shift of absorption spectrum. For the phenyl-substituted acridone derivatives, the UV/vis absorption spectra are slightly blue-shifted in comparison

to the corresponding hexyl-substituted ones, owing to the p - π conjugation of the pending phenyl group (see the supporting information). The corresponding optical energy gaps are in the range of 2.49–3.05 eV, estimated from the onsets of the absorption spectra. The UV/vis absorption of the fused π -extended acridone derivatives was further studied by time-dependent density functional theory (TDDFT) calculation at the B3LYP/6-311G+(2p,d) level of theory in dichloromethane as solvent. The energies of the first excited state are in the range of 2.59–3.33 eV with the HOMO to LUMO transition as the main contribution to the fine structured absorption bands at the long wavelength (see the supporting information).

FULL PAPER

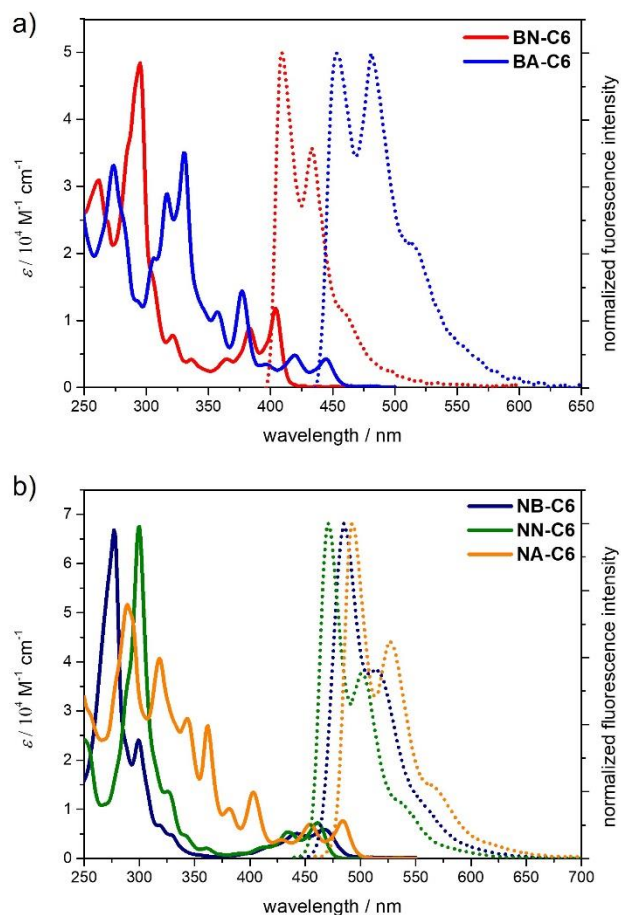


Figure 4. UV/vis absorption and fluorescence emission spectra of the fused π -extended acridone derivatives with hexyl at the amino position measured in dichloromethane at room temperature.

All these acridone derivatives are fluorescent in dichloromethane. For the hexyl-substituted acridone derivatives, compound **BN-C6** shows a nearly same emission spectrum to that of *N*-hexylacridone with the emission maximum at 404 nm.^[5b] However, the absolute quantum yield of **BN-C6** (0.5%) is much lower than that of *N*-hexylacridone (58%) in dichloromethane. The benzene-fused acridone would extend the conjugation in the molecule and should lead to a red-shift of the emission spectra. Again, the unchanged emission spectrum with low intensity of **BN-C6** is related to the reduced conjugation by the steric hindrance induced distortion and the relatively long inner C-C bond at the turning moiety. This is also responsible for the even blue shift of the emission spectrum of **NN-C6** with declined intensity in comparison to that of the linear **NB-C6**. The linear **NB-C6** demonstrates bright green fluorescence with the emission maximum at 485 nm, absolute quantum yield of 52% and relatively long lifetime of 31 ns. Thus the linear extension of acridone would maintain the molecular planarity with a red-shift in both the UV/vis absorption and emission spectra, as well as a good fluorescence intensity. The phenyl-substituted acridone derivatives share the same emission patterns and close intensities to these of the hexyl-substituted ones with a little blue shift in emission positions, which are similar to their UV/vis absorption spectra (see the supporting information). When the solvent was changed to the nonpolar toluene and the polar DMF, the UV/vis absorption and fluorescence emission spectra of each compound are quite similar in patterns with slightly hypsochromic or bathochromic shifts and small Stokes shifts (4-26 nm) (see the supporting information), indicating the quite close structural and electronic properties in the ground states and excited states.

Table 1. Summary of optical and electrochemical properties of the fused π -extended acridone derivatives.

compd.	λ_{ab} ^[a] (nm)	$E_{g,opt}$ ^[b] (eV)	$\lambda_{em}(\lambda_{ex})$ ^[c] (nm)	Φ_F ^[c] (%)	τ ^[c] (ns)	$\lambda_{em}(\lambda_{ex})$ ^[d] (nm)	Φ_F ^[d] (%)	τ ^[d] (ns)	E_{ox1} ^[e] (V)	E_{red1} ^[e] (V)	$E_{g,electro.}$ (eV)	E_{HOMO} ^[f] (eV)	E_{LUMO} ^[g] (eV)
BN-C6	404	2.99	409,433 (383)	0.5	0.63	440,487,519 (383)	4.8	24	0.98	- ^[h]	-	-5.68	-2.69 ^[i]
BN-Ph	397	3.05	402,426 (377)	1.4	0.45	441,486,510 (377)	7.1	3.0	1.03	-2.38	3.06	-5.67	-2.61
BA-C6	445	2.72	454,482 (419)	1.4	4.5	491,516,545 (419)	0.9	42	0.74	-2.20	2.76	-5.44	-2.68
BA-Ph	439	2.74	448,475 (414)	1.1	1.2	504 (414)	0.9	1.8	0.80	-2.17	2.78	-5.49	-2.71
NB-C6	467	2.54	485,514 (442)	52	31	569 (442)	4.9	31	0.79	-2.08	2.68	-5.52	-2.84
NB-Ph	461	2.57	481,507 (435)	66	14	548 (435)	6.5	16	0.93	-2.08	2.73	-5.55	-2.82
NN-C6	461	2.61	471,502 (435)	13	3.0	525 (435)	6.1	3.6	0.80	-2.08	2.68	-5.52	-2.84
NN-Ph	454	2.64	464,494 (429)	14	3.3	523 (429)	0.3	4.0	0.97	-2.06	2.75	-5.58	-2.83
NA-C6	484	2.49	493,527 (454)	6	2.4	550 (454)	4.9	0.6	0.68	-2.04	2.51	-5.36	-2.85
NA-Ph	476	2.52	486,519 (448)	8.4	2.9	539,576(448)	0.9	1.0	0.72	-2.04	2.55	-5.43	-2.88

[a] Absorption at the longest wavelength in dichloromethane at room temperature. [b] Estimated from absorption onset. [c] Measured in dichloromethane at room temperature. [d] Measured in solid state at room temperature. [e] From the DPV measurements in 0.1 M nBu₄NPF₆ dichloromethane solution at room temperature with ferrocene as internal reference. [f] $E_{HOMO} = -(4.8 + E_{ox1,onset})$ eV. [g] $E_{LUMO} = -(4.8 + E_{red1,onset})$ eV. [h] Not observed. [i] $E_{LUMO} = E_{HOMO} + E_{g,opt}$.

FULL PAPER

The fluorescence spectra of the acridone derivatives were measured in the solid state (see the supporting information). The emission maxima are red-shifted in comparison to those measured in the dichloromethane solution due to the close contacts caused excimer coupling.^[21] The absolute quantum yields of the acridone derivatives in the solid state are in the range of 0.3%-7.1%. The fluorescence intensities of **BN-C6** and **BN-Ph** are better than those in the solutions due to the restricted vibrations at the fjord of carbonyl and naphthalene in the solid state.^[22] All the other compounds show decreased quantum yields in the solid state for the excited states of the aggregates decay or relax to the ground state in the nonradiative fashion.^[23]

The redox properties of these acridone derivatives are characterized by cyclic voltammetry (CV) and differential pulse voltammetry (DPV) measurements in dichloromethane. The CV measurements show that all the oxidative waves are irreversible. Irreversible reductive waves are observed for the acridone derivatives starting with methyl 2-bromobenzoate, while the rest ones demonstrate reversible reductive waves. The first oxidative potentials of these acridone derivatives are in the range of 0.68-1.03 V, estimated from the DPV measurement. The HOMO energy level calculated from the onset of the first oxidative wave is -5.68 eV for **BN-C6**, which is raised to -5.36 eV for **NA-C6**. The potential of the first reductive wave is -2.38 V for **BN-Ph** and increases to -2.04 V for **NA-Ph**. The estimated LUMO energy levels ranges from -2.61 eV to -2.88 eV. The corresponding energy gaps from the electrochemical measurements are in the scale of 2.51-3.06 eV, which are in good agreements with their optical energy gaps.

Theoretical calculations

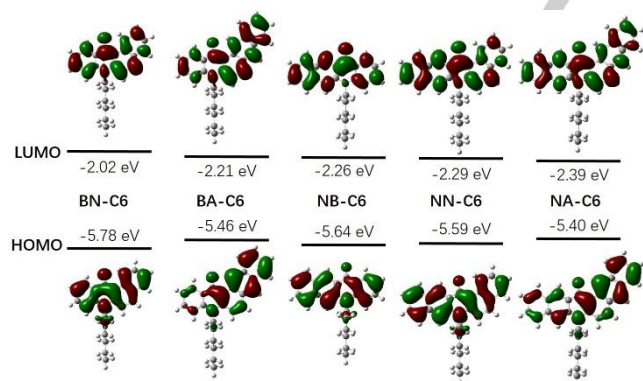


Figure 5. DFT calculated frontier molecular orbitals and energy levels of the fused π -extended acridone derivatives with hexyl at the amino position calculated at the B3LYP/6-311+G (d,p) level of theory.

To investigate the influences of π -extension of acridone on the electronic properties, DFT calculations were carried out at B3LYP/6-311G+(d,p) level of theory in vacuo (Figure 5 and Figure S91). The HOMO and LUMO orbitals are distributed over the whole molecular skeleton of the π -extended acridone. For the *N*-hexylacridone, the HOMO and LUMO energy levels are -5.87 eV and -1.95 eV, respectively, and the corresponding energy gap is 3.92 eV.^[5c] With the increase of π -extension of the acridone derivatives, the frontier molecular orbital energy levels are convergent to -5.40 eV and -2.39 eV for **NA-C6**, which reduces the corresponding energy gap to 3.01 eV. Compared to the

angular acridone derivative, the linear isomer possesses a relatively high HOMO energy level and a low LUMO energy level, thus resulting in a decline in the energy gap. For example, the HOMO and LUMO energy levels of the angular **BN-C6** are -5.78 eV and -2.02 eV, respectively; the corresponding energy levels are changed to -5.64 eV and -2.26 eV for the linear **NB-C6**. Thus, the energy levels of the fused π -extended acridone derivatives can be tuned by changing the manner of fusion and the distance of extension.

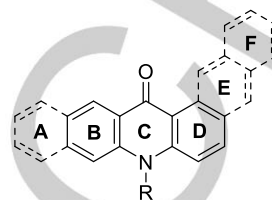


Table 2. NICS(1)_{zz} values of the fused acridone derivatives.^[a]

Compd.	A	B	C	D	E	F
BB-C6	-	-24.1	-4.9	-24.1	-	-
BB-Ph	-	-25.6	-5.6	-25.6	-	-
BN-C6	-	-25.9	-4.6	-20.7	-28.9	-
BN-Ph	-	-26.1	-5.5	-20.7	-29.1	-
BA-C6	-	-25.9	-4.8	-16.4	-32.7	-26.5
BA-Ph	-	-26.1	-5.5	-16.3	-32.8	-26.6
NB-C6	-25.9	-27.1	-1.3	-24.3	-	-
NB-Ph	-26.0	-27.6	-1.9	-24.6	-	-
NN-C6	-25.2	-26.9	-2.9	-18.9	-28.1	-
NN-Ph	-26.1	-28.4	-2.8	-19.8	-28.6	-
NA-C6	-25.5	-26.9	-2.9	-14.8	-31.4	-26.2
NA-Ph	-26.2	-28.4	-2.8	-15.7	-32.3	-26.3

[a] Calculated at the GIAO/DFT/B3LYP/6-311+G(d) level of theory. For comparison, the NICS(1)_{zz} values of *N*-hexylacridone (**BB-C6**) and *N*-phenylacridone (**BB-Ph**) are also calculated.

Since the crystal structural analysis reveals the presence of relatively longer and shorter C-C bonds in the benzene ring at the turning points of the angularly fused acridone derivatives, their aromaticities were studied by the nucleus-independent chemical shift (NICS) calculations (Table 2).^[24] All the benzene rings in the acridone derivatives are aromatic according to the NICS(1)_{zz} values. However, the aromaticity of benzene ring D at the turning point of the angularly fused acridone derivatives is weakened when more benzene rings are fused. This is consistent with the crystal structural analysis. The pyridone ring C possesses a weak aromatic character, which is probably caused by the intramolecular charge transfer induced electron delocalization over the pyridone ring and can be easily recognized when its corresponding resonance structure of acridine is considered, as supposed in the crystal structure analysis.

The π -extended acridone derivatives possess the similar structures to polyacenes and have potential applications as photoelectronic materials.^[14] Considering the presence of face-to-face π - π stackings in the crystals, the charge transport property

FULL PAPER

was preliminarily evaluated via the equation based on the Marcus theory and hopping mechanism.^[25] According to the previously investigations, such theoretical calculation is reliable in studying the charge transport property.^[12b,26]

$$\mu = \frac{e\pi d^2 t^2}{k_B T h} \left(\frac{\pi}{\lambda k_B T} \right)^{1/2} \exp\left(-\frac{\lambda}{4k_B T}\right)$$

Here, e , k_B , h and T are the electron charge, Boltzmann constant, Planck constant and temperature, respectively. d is the center-of-mass distance in the charge transfer direction and can be obtained from the molecular π - π stackings in the crystal. λ is the reorganization energy and is defined as the energy required to reorganize the molecular geometry from initial to final coordinates.^[25b,27] t is the transfer integral and is sensitive to the mode of packing.^[25b,28] Thus the two molecules of π - π stacking in the crystal were used directly without the optimization of geometry. All the calculations were carried out at the B3LYP/6-311G+(d,p)

level of theory and both the hole and electron transports were considered. The calculated results are listed in Table 3.

The calculations reveal that all the fused acridone derivatives possess comparable and even larger hole reorganization energy in comparison to that of *N*-phenylacridone **BB-Ph**. But for the electron reorganization energy, the acridone derivatives that are synthesized starting from benzoate ester give relatively higher reorganization energies than that of **BB-Ph**, whereas the other ones have lower reorganization energies. Moreover, the reorganization energies for hole transports are lower than those for electron transports, making these acridone derivatives more suitable as hole transports materials. When the transfer integral is concerned, the linearly fused acridone derivatives **NB-C6** and **NB-Ph** demonstrate the largest values of electronic coupling, 131.6 meV and 146.3 meV, respectively. These values are much higher than those of their congener rubrene ($t_h = 100$ meV and $t_e = 53$ meV).^[29]

Table 3. Summary of the calculated hole and electron mobilities of acridone derivatives at 300 K.^[a]

Compd.	λ_h (meV)	t_h (meV)	λ_e (meV)	t_e (meV)	d (Å)	μ_h (cm ² V ⁻¹ s ⁻¹)	μ_e (cm ² V ⁻¹ s ⁻¹)
BN-C6	137.8	35.8	271.8	32.4	4.94	0.72	0.12
BN-Ph	126.7	63.3	250.9	93.3	4.09	1.79	0.83
BA-C6	172.0	33.3	255.4	77.8	4.09	0.27	0.55
BA-Ph	174.3	84.5	251.7	125.6	3.38	1.17	1.02
NB-C6	101.1	131.6	193.6	89.7	4.62	14.2	1.95
NB-Ph-a	113.3	15.1	195.3	128.3	3.84	0.11	2.69
NB-Ph-b	113.3	75.0	195.3	146.3	5.43	5.33	7.00
NN-C6	89.8	3.7	171.0	114.4	3.61	0.008	2.56
NN-Ph-a	98.5	16.9	169.8	105.0	3.73	0.16	2.33
NN-Ph-b	98.5	24.5	169.8	84.5	3.78	0.34	1.55
NA-C6-a	125.8	10.6	176.9	55.0	3.73	0.04	0.59
NA-C6-b	125.8	5.2	176.9	19.5	6.32	0.03	0.21
NA-Ph-a	128.6	12.2	175.8	58.1	3.59	0.05	0.61
NA-Ph-b	128.6	24.8	175.8	73.5	5.21	0.43	2.07
BB-Ph	91.8	23.5	240.8	2.6	3.82	0.35	0.0006

[a] All the calculations were carried out at the B3LYP/6-311+G(d,p) level of theory.

Based on the reorganization energy, transfer integral and the center-of-mass distance, the hole and electron mobilities of acridone derivatives are calculated by setting the temperature at 300 K. The hole and electron mobilities of the parent *N*-phenylacridone **BB-Ph** are estimated to be 0.35 cm²V⁻¹s⁻¹ and 0.0006 cm²V⁻¹s⁻¹, respectively, according to its crystal packings.^[30] When more benzene rings are fused to acridone, the mobility varies according to the molecular shape and *N*-substituents. The acridone derivatives with one side containing benzene ring demonstrate better hole mobilities than those with one side bearing linearly fused naphthalene. However, the latter ones show the relatively better electron mobilities than those of

the former ones. The *N*-substitution with phenyl lead to better mobilities than those with hexyl, except the electron mobility of **NN-Ph**, which is slightly lower than that of **NN-C6**. The linear compounds **NB-C6** and **NB-Ph** exhibit good transfer integrals, thus resulting the best hole and electron mobilities of 14.2 cm²V⁻¹s⁻¹ and 7.00 cm²V⁻¹s⁻¹, respectively, which are much higher than those of **BB-Ph**, even with relatively farther center-of-mass distances. However, it is worthwhile to note that the π - π stackings of **NB-C6** are not continuous in the crystal, which will affect the intermolecular electronic coupling. For compounds **NB-Ph**, **NN-Ph**, **NA-C6** and **NA-Ph** with consecutive π -stackings in the crystals, their charge transports are determined by the two

FULL PAPER

molecules packed with related lower mobilities in the range of 0.21-2.69 $\text{cm}^2\text{V}^{-1}\text{s}^{-1}$ for electron transports and 0.03-0.43 $\text{cm}^2\text{V}^{-1}\text{s}^{-1}$ for electron transports.

Conclusion

In summary, the fused π -extended acridone derivatives were synthesized via the acid-promoted cyclization of *N*-aryltrianilic ester and the theoretical calculations revealed that the favored angular acridone derivative was formed through a relatively lower reaction activation energy to generate a more thermodynamically stable intermediate. The single crystal structural analysis showed the formation of π - π stackings along the linear acridone moiety. However, the C-H... π interaction of flexible hexyl chain and the aromatic surface interfered the continuous π - π stackings in the crystals. The linearly fused acridone **NB-C6** overlapped each other so well that it dimerized in the crystalline state at the ambient condition after a long time storage. For the phenyl-substituted fused acridone derivatives, the pending phenyl group plays an important role in directing the molecular packing in the crystals via the formation of intermolecular hydrogen bonds between the oxygen atom of carbonyl and the hydrogen atom of the pending phenyl group. The benzene ring at the turning point of the angularly fused acridone derivatives contains the relatively long and short C-C bonds, which reduces the conjugation of the whole molecule and is also reflected in the UV/vis absorption and fluorescence emission spectra, as well as the weakened aromaticity. The mobility calculation reveals that benzene and naphthalene fused π -extended acridone derivatives, especially the linearly fused ones, are good candidates of organic functional materials with potential applications in electronic devices.

Acknowledgements

We are grateful for the financial support from the Jiangsu Specially Appointed Professor Plan.

Keywords: acridone • aromaticity • conjugation • nitrogen heterocycles • polycyclic aromatic hydrocarbons

- [1] M. Stepień, E. Gońska, M. Żyła, N. Sprutta, *Chem. Rev.* **2017**, *117*, 3479-3716.
- [2] a) J. H. Rothman, W. C. Still, *Bioorg. Med. Chem. Lett.* **1999**, *9*, 509-512; b) P. Nikolov, I. Petkova, G. Köler, S. Stojanov, *J. Mol. Struct.* **1998**, *448*, 247-254.
- [3] a) P. Pander, A. Swist, R. Motyka, J. Soloducho, F. B. Diasa, P. Data, *J. Mater. Chem. C* **2018**, *6*, 5434-5443; b) Q. T. Siddiqui, A. A. Awasthi, P. Bhui, M. Muneer, K. R. S. Chandrakumar, S. Bose, N. Agarwal, *J. Phys. Chem. C* **2019**, *123*, 1003-1014; c) R. Liu, W. Ding, Q. Zhang, Y. Song, G. Zhang, *ChemistrySelect* **2019**, *4*, 10536-10542.
- [4] a) K. D. Thériault, C. Radford, M. Parvez, B. Heyne, T. C. Sutherland, *Phys. Chem. Chem. Phys.* **2015**, *17*, 20903-20911; b) B. K. Sharma, A. M. Shaikh, N. Agarwal, R. M. Kamble, *RSC Adv.* **2016**, *6*, 17129-17137.
- [5] a) W.-C. Chow, G.-J. Zhou, W.-Y. Wong, *Macromol. Chem. Phys.* **2007**, *208*, 1129-1136; b) R. Liu, G. Zhu, Y. Ji, G. Zhang, *Eur. J. Org. Chem.* **2019**, 3217-3223.
- [6] D. A. Vezzu, J. C. Deaton, M. Shayeghi, Y. Li, S. Huo, *Org. Lett.* **2009**, *11*, 4310-4313.
- [7] R. Liu, H. Gao, L. Zhou, Y. Ji, G. Zhang, *ChemistrySelect* **2019**, *4*, 7797-7804.
- [8] a) Q. Qi, J. Qian, X. Tan, J. Zhang, L. Wang, B. Xu, B. Zou, W. Tan, *Adv. Funct. Mater.* **2015**, *25*, 4005-4010; b) S. Jiang, J. Wang, Q. Qi, J. Qian, B. Xu, F. Li, Q. Zhou, W. Tian, *Chem. Commun.* **2019**, 55, 3749-3752; c) R. Liu, G. Zhu, G. Zhang, *RSC Adv.* **2020**, *10*, 7092-7098.
- [9] W. Chen, S. Wang, G. Yang, S. Chen, K. Ye, Z. Hu, Z. Zhang, Y. Wang, *J. Phys. Chem. C* **2016**, *120*, 587-597;
- [10] M. Krick, J. J. Holstein, A. Wuttke, R. A. Mata, G. H. Clever, *Eur. J. Org. Chem.* **2017**, 5141-5146.
- [11] a) T. Suzuki, H. Okada, T. Nakagawa, K. Komatsu, C. Fujimoto, H. Kagi, Y. Matsuo, *Chem. Sci.* **2018**, *9*, 475-482; b) Y. Matsuo, Y. Wang, H. Ueno, T. Nakagawa, H. Okada, *Angew. Chem. Int. Ed.* **2019**, *58*, 8762-8767; *Angew. Chem.* **2019**, *131*, 8854-8859;
- [12] a) K. Yamamoto, S. Higashibayashi, *Chem. Eur. J.* **2016**, *22*, 663-671; b) M. Mamada, O. Inada, T. Komino, W. J. Potscavage, Jr., H. Nakanotani, C. Adachi, *ACS Cent. Sci.* **2017**, *3*, 769-777; c) Y.-Y. Jin, Q. Fang, *J. Org. Chem.* **2019**, *84*, 3832-3842; d) N. Deng, G. Zhang, *Org. Lett.* **2019**, *21*, 5248-5251; e) L. Zhou, G. Zhang, *Angew. Chem. Int. Ed.* **2020**, *59*, 8963-8968; *Angew. Chem.* **2020**, *132*, 9048-9053.
- [13] a) I. Sungwienwong, J. J. Ferrie, J. V. Jun, C. Liu, T. M. Barrett, Z. M. Hostetler, N. Ieda, A. Hendricks, A. K. Muthusamy, R. M. Kohli, D. M. Chenoweth, G. A. Petersson, E. James Petersson, *J. Phys. Org. Chem.* **2018**, *31*, e3813; b) W. Zhang, K. F. Koehler, B. Harris, P. Skolnick, J. M. Cook, *J. Med. Chem.* **1994**, *37*, 745-757; c) A. F. F. da Silva, R. S. G. R. Seixas, A. M. S. Silva, J. Coimbra, A. C. Fernandes, J. P. Santos, A. Matos, J. Rino, I. Santos, F. Marques, *Org. Biomol. Chem.* **2014**, *12*, 5201-5211; d) S. Thamaraiselvi, P. S. Mohan, *Z. Naturforsch. B: Chem. Sci.* **1999**, *54*, 1337-1341; e) R. S. G. R. Seixas, A. M. S. Silva, D. C. G. A. Pinto, J. A. S. Cavaleiro, *Synlett* **2008**, 3193-3197; f) L. Jayabalan, P. Shanmugam, *Synthesis* **1991**, 217-220.
- [14] a) J. E. Anthony, *Chem. Rev.* **2006**, *106*, 5028-5048; b) J. E. Anthony, *Angew. Chem. Int. Ed.* **2008**, *47*, 452-483; *Angew. Chem.* **2008**, *120*, 460-492; c) S. S. Zade, M. Bendikow, *Angew. Chem. Int. Ed.* **2010**, *49*, 4012-4015; *Angew. Chem.* **2010**, *122*, 4104-4107; d) U. H. F. Bunz, J. U. Engelhart, B. D. Lindner, M. Schaffroth, *Angew. Chem. Int. Ed.* **2013**, *52*, 3810-3821; *Angew. Chem.* **2013**, *125*, 3898-3910; e) Q. Ye, C. Chi, *Chem. Mater.* **2014**, *26*, 4046-4056; f) H. F. Bettinger, C. Tçnshoff, *Chem. Rec.* **2015**, *15*, 364-369; g) U. H. F. Bunz, *Acc. Chem. Res.* **2015**, *48*, 1676-1686; h) U. H. F. Bunz, J. Freudenberg, *Acc. Chem. Res.* **2019**, *52*, 1575-1587; i) M. Müller, L. Ahrens, V. Brosius, J. Freudenberg, U. H. F. Bunz, *J. Mater. Chem. C* **2019**, *7*, 14011-14034.
- [15] a) Allen, C. F. H. McKee, G. H. W. *Org. Syn.* **1939**, *19*, 6-8; b) S. L. MacNeil, M. Gray, L. E. Briggs, J. J. Li, V. Snieckus, *Synlett* **1998**, 419-421; c) R. Nishio, S. Wessely, M. Sugiura, S. Kobayashi, *J. Comb. Chem.* **2006**, *8*, 459-461; d) J. Zhao, R. C. Larock, *J. Org. Chem.* **2007**, *72*, 583-588; e) S. L. MacNeil, M. Gray, D. G. Gusev, L. E. Briggs, V. Snieckus, *J. Org. Chem.* **2008**, *73*, 9710-9719; f) J. Huang, C. Wan, M.-F. Xu, Q. Zhu, *Eur. J. Org. Chem.* **2013**, 1876-1880; g) P.-C. Huang, K. Parthasarathy, C.-H. Cheng, *Chem. Eur. J.* **2013**, *19*, 460-464; h) Z. Xiong, X. Zhang, Y. Li, X. Peng, J. Fu, J. Guo, F. Xie, C. Jiang, B. Lin, Y. Liu, M. Cheng, *Org. Biomol. Chem.* **2018**, *16*, 7361-7374; i) J. Janke, A. Villinger, P. Ehlers, P. Langer, *Synlett* **2019**, 30, 817-820.
- [16] M. J. Frisch, G. W. Trucks, H. B. Schlegel, G. E. Scuseria, M. A. Robb, J. R. Cheeseman, G. Scalmani, V. Barone, G. A. Petersson, H. Nakatsuji, X. Li, M. Caricato, A. V. Marenich, J. Bloino, B. G. Janesko, R. Gomperts, B. Mennucci, H. P. Hratchian, J. V. Ortiz, A. F. Izmaylov, J. L. Sonnenberg, D. Williams-Young, F. Ding, F. Lipparini, F. Egidi, J. Goings, B. Peng, A. Petrone, T. Henderson, D. Ranasinghe, V. G. Zakrzewski, J. Gao, N. Rega, G. Zheng, W. Liang, M. Hada, M. Ehara, K. Toyota, R. Fukuda, J. Hasegawa, M. Ishida, T. Nakajima, Y. Honda, O. Kitao, H. Nakai, T. Vreven, K. Throssell, J. A. Montgomery, Jr., J. E. Peralta, F. Ogliaro, M. J. Bearpark, J. J. Heyd, E. N. Brothers, K. N. Kudin, V. N. Staroverov, T. A. Keith, R. Kobayashi, J. Normand, K. Raghavachari, A. P. Rendell, J. C. Burant, S. S. Iyengar, J. Tomasi, M. Cossi, J. M. Millam, M. Klene, C. Adamo, R. Cammi, J. W. Ochterski, R. L. Martin, K. Morokuma, O. Farkas, J. B. Foresman, and D. J. Fox, *Gaussian 16, Revision A.03*, Gaussian, Inc., Wallingford CT, **2016**.
- [17] CCDC 2003932-2003942 contain the supplementary crystallographic data for this paper. These data can be obtained free of charge from The Cambridge Crystallographic Data Centre.

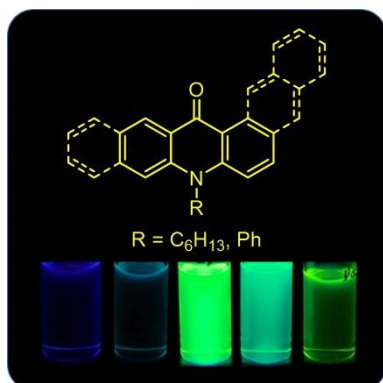
FULL PAPER

- [18] F. H. Allen, O. Kennard, D. Watson, L. Brammer, A. G. Orpen, R. Taylor, *J. Chem. Soc., Perkin Trans. 2* **1987**, S1-S19.
- [19] a) O. Ermer, J. Neudörfl, *Helv. Chim. Acta* **2001**, *84*, 1268-1313; b) J. Buche, T. Wurm, S. Taschinski, E. Sachs, D. Ascough, M. Rudolph, F. Rominger, A. S. K. Hashmi, *Adv. Synth. Catal.* **2017**, *359*, 225-233.
- [20] a) H. Bouas-Laurent, A. Castellan, J.-P. Desvergne, R. Lapouyade, *Chem. Soc. Rev.* **2000**, *29*, 43-55; b) H. Bouas-Laurent, A. Castellan, J.-P. Desvergne, R. Lapouyade, *Chem. Soc. Rev.* **2001**, *30*, 248-263; c) B. Purushothaman, S. R. Parkin, J. E. Anthony, *Org. Lett.* **2010**, *12*, 2060-2063; d) J. U. Engelhart, B. D. Lindner, O. Tverskoy, F. Rominger, U. H. F. Bunz, *Chem. Eur. J.* **2013**, *19*, 15089-15092.
- [21] A. Slodek, A. Maroń, M. Pająk, M. Matussek, I. Grudzka-Flak, J. G. Malecki, A. Świtlicka, S. Krompiec, W. Danikiewicz, M. Grela, I. Gryca, M. Penkala, *Chem. Eur. J.* **2018**, *24*, 9622-9631.
- [22] J. Mei, N. L. C. Leung, R. T. K. Kwok, J. W. Y. Lam, B. Z. Tang, *Chem. Rev.* **2015**, *115*, 11718-11940.
- [23] Q. Wu, T. Zhang, Q. Peng, D. Wang, Z. Shuai, *Phys. Chem. Chem. Phys.* **2014**, *16*, 5545-5552.
- [24] a) Z. Chen, C. S. Wannere, C. Corminboeuf, R. Puchta, P. v. R. Schleyer, *Chem. Rev.* **2005**, *105*, 3842-3888; b) H. Fallah-Bagher-Shaidaei, C. S. Wannere, C. Corminboeuf, R. Puchta, P. v. R. Schleyer, *Org. Lett.* **2006**, *8*, 863-866.
- [25] a) R. A. Marcus, *Rev. Mod. Phys.* **1993**, *65*, 599-610; b) V. Balzani, A. Juris, M. Venturi, S. Campagna, S. Serroni, *Chem. Rev.* **1996**, *96*, 759-833.
- [26] W.-Q. Deng, L. Sun, J.-D. Huang, S. Chai, S.-H. Wen, K.-L. Han, *Nat. Protoc.* **2015**, *10*, 632-642.
- [27] a) V. Lemaire, D. A. da Silva Filho, V. Coropceanu, M. Lehmann, Y. Geerts, J. Piris, M. G. Debije, A. M. van de Craats, K. Senthilkumar, L. D. A. Siebbeles, J. M. Warman, J.-L. Brédas, J. Cornil, *J. Am. Chem. Soc.* **2004**, *126*, 3271-3279; b) M.-X. Zhang, G.-J. Zhao, *J. Phys. Chem. C* **2012**, *116*, 19197-19202; c) X. Liu, M. Li, R. He, W. Shen, *Phys. Chem. Chem. Phys.* **2014**, *16*, 311-323.
- [28] a) V. Coropceanu, J. Cornil, D. A. da Silva Filho, Y. Olivier, R. Silbey, J.-L. Brédas, *Chem. Rev.* **2007**, *107*, 926-952; b) E. F. Valeev, V. Coropceanu, D. A. da Silva Filho, S. Salman, J.-L. Brédas, *J. Am. Chem. Soc.* **2006**, *128*, 9882-9886; c) L. Ueberricke, D. Holub, J. Kranz, F. Rominger, M. Elstner, M. Mastalerz, *Chem. Eur. J.* **2019**, *25*, 11121-11134.
- [29] K. A. McGarry, W. Xie, C. Sutton, C. Risko, Y. Wu, V. G. Young, J.-L. Brédas, C. D. Frisbie, C. J. Douglas, *Chem. Mater.* **2013**, *25*, 2254-2263.
- [30] V. E. Zavodnik, L. A. Chetkina, G. A. Val'kova, *Kristallografiya* **1981**, *26*, 392-395.

FULL PAPER

Entry for the Table of Contents

Aromatic systems



The angularly and linearly fused acridone derivatives were synthesized and their properties were shape-dependent. The angularly fused acridone derivatives showed weakened aromaticity of the benzene ring at the turning point, whereas the linearly fused ones demonstrated stronger fluorescence intensity and better electronic couplings with potential applications in organic electronics.